Single Cell Fluorescence Imaging Using Metal Plasmon-Coupled Probe

Jian Zhang, Yi Fu, and Joseph R. Lakowicz*

Center for Fluorescence Spectroscopy, University of Maryland School of Medicine, Department of Biochemistry and Molecular Biology, 725 West Lombard Street, Baltimore, Maryland 21201. Received October 27, 2006; Revised Manuscript Received February 5, 2007

This work constitutes the first fluorescent imaging of cells using metal plasmon-coupled probes (PCPs) at single cell resolution. *N*-(2-Mercapto-propionyl)glycine-coated silver nanoparticles were synthesized by reduction of silver nitrate using sodium borohyride and then succinimidylated via ligand exchange. Alexa Fluor 647-labeled concanavalin A (con A) was chemically bound to the silver particles to make the fluorescent metal plasmon-coupled probes. The fluorescence images were collected using a scanning confocal microscopy. The fluorescence intensity was observed to enhance 7-fold when binding the labeled con A on a single silver particle. PCPs were conjugated on HEK 293 A cells. Imaging results demonstrate that cells labeled by PCPs were 20-fold brighter than those by free labeled con A.

INTRODUCTION

Molecular fluorescence imaging techniques play critical roles in the early detection, diagnosis, and treatment of disease, as well as aid in the studies of biological and biochemical mechanisms, immunology, and neuroscience on single cells (*1*– *4*). Generally, an imaging agent consists of an organic fluorophore moiety and a targeting functionality, such as an antibody, peptide, DNA, or a special ligand (*5*–*7*). However, most imaging agents have several limitations: complicated preparation, strong signal background, fast photobleaching, and single color.

Recently, the use of fluorescently labeled metal particles has become attractive due to near-field interaction of the fluorophore with metal particles (*8*–*17*). The metal particle with the subwavelength size usually displays an energy resonance arising from the collective oscillation of migrated electrons on its surfaces (*18*, *19*), which is defined as plasmon resonance. The wavelength of plasmon resonance is closely relevant to the metal core including metal species, core size, and core shape as well as the dielectric properties of coating layer (*19*–*21*). The fluorophore can be described as an oscillating dipole to radiate energy during fluorescence occurrence (*22*). When it is localized near the metal particle, the radiating energy is dramatically altered through coupling with the metal plasmon resonance to cause a change of the emission properties, which is defined as radiative decay engineering (RDE) (*23*–*25*). Generally, RDE can lead to an enhancement of intensity to be 10^1 to 10^3 times depending upon both the fluorophore and metal core factors as well as the distance between them. Besides the intensity enhancement, the near field interaction of fluorophore with the metal particle can also result in its shorter lifetime (*26*), which leads to less time for the photochemistry while in the excited-state and thus more excitation–emission cycles prior to photobleaching. Hence, the fluorophore usually displays a better photostability near the metal particle (*27*).

The metal particle is known to have large surface area, good chemical stability, and homogeneous dispersion in solution (*28*– *30*). The development of surface chemistry can enable versatile decoration of fluorophores as well as provide targeting functionalities on the metal particle (*31*, *32*). Hence, we can use the dye-labeled metal particle as a novel fluorescence imaging agent to satisfy our specific requirements in the measurements. Because the optical properties of dye-labeled metal particles can be controlled well by the metal plasmon resonance as discussed above, we define it as metal plasmon-coupled probe (PCP). PCP is suggested to be able to offer easier preparation, higher brightness, better photostability, and multiple colors as a new generation of fluorescence imaging agent (*22*, *23*). In this paper, we are concerned with developing a method to make PCPs and label cells using these PCPs. The fluorescence images by PCPs were collected using scanning confocal microscopy at the single cell level and compared with those by unmodified fluorophores.

Dye-labeled concanavalin A (abbreviated as con A) can bind to sugars residing on the cell membrane (*33*–*35*), so it is commonly used in cell labeling in culture (*36*, *37*). In this study, the dye-labeled con A was chemically bound to the silver particle to generate PCP (Scheme 1). The silver particle was synthesized in a typical protocol by reduction of silver salt (*28*). In order to bind con A, the metal particle was functionalized by succinimidyl ester at a terminal position via ligand exchange (*30*, *38*). The con A was bound to the succinimidylated particle by condensation between the succinimidyl ester on the metal particle and the lysine residual on the protein molecule. Alexa Fluor 647-labeled con A was used in the study because of its efficient enhancement as a near-infrared fluorophore near the metal substrate (*39*). HEK 293 A cell line, which is originally derived from human embryonic kidney and utilized frequently in *in vivo* imaging (*40*, *41*), was conjugated by PCPs, and the fluorescence imaging was monitored using confocal microscopy.

EXPERIMENTAL PROCEDURES

All reagents and spectroscopic grade solvents were used as received from Fisher or Aldrich. Alexa Fluor 647-labeled concanavalin A (con A) was commercially available from Molecule Probes. HEK293 A cell line was from Invitrogen. RC dialysis membrane (MWCO 50 000) was purchased from Spectrum Laboratories, Inc. Nanopure water (>18.0 MΩ cm) purified using Millipore Milli-Q gradient system was used in all experiments.

Preparation of Tiopronin-Coated Silver Nanoparticles. *N*-(2-Mercaptopropionyl)glycine (abbreviated as tiopronin)-

Scheme 1. Tiopronin-Coated Silver Particles Were Succinimidylated via Ligand Exchange and Then Chemically Bound by Alexa Fluor 647-Labeled Con A via Condensation

coated silver nanoparticles were prepared using a modified Brust reaction with a mole ratio of tiopronin/silver nitrate = 1/6 in methanol using an excess amount of sodium borohydride as reducing agent (*42–44*). Removal of the solution by filtration, the residual precipitated solid was washed with methanol and acetone, respectively, to obtain the metal particles. The particles (1 mg/mL) and tiopronin (10 mM) were codissolved in water, and the solution was stirred for 24 h to anneal the particles (*45, 46*). The water was removed under vacuum and the residue was washed thoroughly with methanol and acetone. The solid tiopronin-coated particles were further purified through dialysis against water (MWCO 50 000).

Functionalization of Silver Particles. (2-Mercapto-propionylamino)acetic acid 2,5-dioxo-pyrrolidin-1-yl ester was synthesized as previously reported (*47*). A 4×10^{-8} mol amount of this compound was codissolved with a 4×10^{-8} mol amount of tiopronin-coated silver particles in water and stirred for 72 h at room temperature for ligand exchange. Some tiopronin molecules were expected to be displaced by the succinimidyl ester molecules on the metal cores in a mole ratio of 1/1 (*38*). Unbound compounds were removed by dialysis against water (MWCO 50 000), and the resultant metal particles were obtained under vacuum.

Binding con A onto Silver Particles. Alexa Fluor 647-labeled concanavalin A (con A) was chemically bound on the succinimidylated metal particle by condensation between the terminal succinimidyl ester on the metal particle and the lysine residue on the con A (*35, 36*). The metal particles (2×10^{-8} M) and dye-labeled con A (2×10^{-8} M) were codissolved in molar ratio of 1/1 in water and stirred for 2 h at room temperature. One drop of ammonia was added to the solution to block the nonreacting succinimidyl ester on the metal particle. The solution was centrifuged at 5000 rpm/s to remove the aggregates in the reaction and then dialyzed against 10 mM glucose–BAS buffer solution to remove the impurities.

Conjugating Dye-Labeled con A and PCPs on Cell Lines. HEK293 A cell lines were suspended in 500 μL aliquots of 250 g/mL con A solutions made in 0.01 M PBS buffer (pH = 7.2) and agitated for 1 h at room temperature (*37*). PCPs were incubated with the cells at the same fluorophore concentration and for the same incubation time as the unmodified dye-labeled con A. All cell samples were washed three times with PBS buffer solution before using imaging measurements.

Spectra and Imaging Measurements. Absorption spectra were monitored with a Hewlett-Packard 8453 spectrophotometer. Ensemble fluorescence spectra were recorded with a Cary Eclipse Fluorescence Spectrophotometer. Transmission electron micrographs (TEM) were taken with side-entry Philips electron microscopy at 120 keV. Samples were cast from water solutions onto standard carbon-coated (200–300 Å) Formvar films on copper grids (200 mesh) by placing a droplet of a 10-fold diluted aqueous sample solution on the grids. The size distribution of the metal core was analyzed with Scion Image Beta Release 2 counting at least 200 particles. For fluorescence imaging measurements, the diluted samples were dispersed on a precleaned glass coverslip. The coverslips (18 × 18 μm, Corning)

were first soaked in a 10:1 (v:v) mixture of concentrated H_2SO_4 and 30% H_2O_2 overnight, thoroughly rinsed with water, sonicated in absolute ethanol, and dried with an air stream. All the single-molecule measurements were performed using time-resolved confocal microscopy (MicroTime 200, PicoQuant). Briefly, it consists of an inverted confocal microscope coupled to a high-sensitivity detection setup. A single mode pulsed laser diode (635 nm, 100 ps, 40 MHz) (PDL800, PicoQuant) was used as the excitation light. An oil immersion objective (Olympus, 100×, 1.3NA) was used both for focusing laser light onto the sample and collecting fluorescence emission from the sample. The fluorescence that passed a dichroic mirror (Q655LP, Chroma) was focused onto a 75 μm pinhole for spatial filtering to reject out-of-focus signals. The emission signals were discretely focused onto single photon avalanche diodes (SPAD) (SPCM-AQR-14, Perkin-Elmer Inc). The data collected using the TimeHarp 200 board was stored in the time-tagged time-resolved mode (TTTR), recording every detected photon with its individual timing, which is the basis for the following single-molecule analysis.

RESULTS AND DISCUSSION

The tiopronin-coated silver particles displayed a typical silver plasmon absorbance at 405 nm in water (Figure 1) (*43*). The average diameter of the metal cores was 20 nm as measured from 200 transmission electron micrographs images (TEM, Figure 2a), and their *average* chemical compositions were estimated to be ca. $(Ag)_{2.5 \times 105}(Tio)_{5.0 \times 103}$. The silver particles were succinimidylated via ligand exchange using (2-mercapto-propionylamino)acetic acid 2,5-dioxo-pyrrolidin-1-yl ester. Typically, such ligand exchange occurs in a molar ratio of 1/1 on the surface of metal particles according to Murray et al. (*38*), so we suggest that there exists average one succinimidyl ligand on each metal particle even though the ligand exchange is completely accomplished. The reason for one succinimidyl ester ligand/per particle is to compare the cell imaging by PCPs and unmodified con A at the same quantity of fluorophore. In future work, we can conjugate more dye-labeled con A molecules to
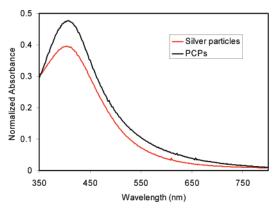

Figure 1. Normalized absorbance spectra of tiopronin-coated silver particle and con A-bound silver particles in water.

Figure 2. Transmission electron micrographs (TEM) images of (A) tiopronin-coated silver particles and (B) con A-bound particles.
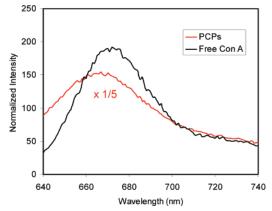

Figure 3. Ensemble fluorescence spectra of Alexa 647-labeled con A and con A-bound silver particle in water.

get PCPs with higher brightness and more capability to capture on the membranes of cells.

Alexa Fluor 647-labeled con A was chemically bound to the silver particle via condensation reaction (Scheme 1). Because only one succinimidyl ester was expected to bind per metal particle, each metal particle was bound maximally by one con A molecule. No significant cross-linking was observed from TEM images (Figure 2b). Even if cross-linking had occurred in the con A binding, the aggregate was removed by the centrifugation. The con A-bound silver particles, so-called PCPs, displayed a blue-shifting of fluorescence wavelength from 672 to 667 nm with the binding, accompanied by simultaneous band broadening (Figure 3). However, the binding did not alter the metal plasmon absorbance (Figure 1), which was principally due to the limitation of the con A amount on each metal particle. This result is consistent with what we require for PCPs in this case.

In order to obtain the exact amount of con A on each metal particle, the metal cores of PCPs (1×10^{-6} M) were removed by adding dropwise sodium cyanide (*32*). The concentration of con A in the residual solution was measured to be 8×10^{-7} M

according to the fluorescence intensity. Hence, the molar ratio of bound con A/metal particle was estimated to be 0.8, showing that one metal particle was bound by less than one con A. TEM images of PCPs (Figure 2b) displayed an insignificant change from the tiopronin-coated particles (Figure 2a), indicating that the above surface reactions did not obviously influence the metal core. Furthermore, TEM results also confirmed that there was not significant cross-linking between the metal particles and con A molecules as described earlier.

Fluorescence images were collected by scanning confocal microscopy. Tiopronin-coated silver particles displayed light-scattering images with typical photoblinking behavior, which take on 'streaky" appearances and the spots no longer appear as full and round shapes (Figure 4a). The streaks are not noise, having intensity levels significantly greater than the background. The strong blinking behavior may arise from temporal variations in the emission rate during illumination, most likely from strong "nondestructive" silver blinking as confirmed by our previous result (*48*). Contrarily, full and round spots were observed from the unmodified con A with an average intensity at 50 kHz (Figure 4b). A representative time trace was given as gradual intensity decay (Figure 5), indicating that each con A molecule consists of multiple dye molecules. After binding con A to the silver particle, the fluorescence of PCPs became more intense (Figure 4c), about 7 fold brighter than that of unmodified con A. This enhancement efficiency is in good agreement with the value obtained from the ensemble spectra in solution (6 fold). Most of the unmodified con A molecules were bleached away within 15 s (Figure 5), while at least half of the PCPs were monitored indefinitely without photobleaching, implying that the fluorophores on the metal particles became more photostable. Enhanced brightness and lengthened photostability are typical properties of metal-enhanced fluorescence as in our previous description (*24, 25*).

HEK293 A cell lines were conjugated with either unmodified con A or PCPs. The imaging was monitored with confocal microscopy at the single cell level (Figure 6). At least 50 images were collected for each sample. Although the cells were measured under dry conditions, the averaged size of the HEK293 A cells was in the range of $5-10$ μm, close to those of living cells on a glass substrate, reported by Zeng, et al. (*49*). It was difficult to distinguish the individual bright spots on the cells, implying that the probes were packed densely on the cell membranes in both situations. The brightness was analyzed on the basis of the average value of the cell images. It is shown that the image brightness of cells by unmodified con A (Figure 6d,e) is identical to that of free unmodified con A (Figure 4b), implying that the conjugation cannot significantly alter the brightness of the probe on the cell. However, the image brightness of cells labeled by PCPs (Figure 6a–c) is 20-fold greater than that of free unmodified con A. Theses images by PCPs are even 4-fold brighter than those by unconjugated PCPs, which is most likely attributed to the coupling effect of PCPs on the cell membrane (*42*).
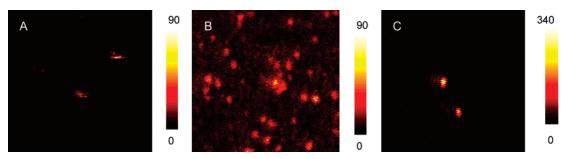

Figure 4. Scattering/fluorescence images (a) tiopronin-coated silver particles, (b)Alexa Fluor 647 labeled con A, and (c) con A-bound silver particles.
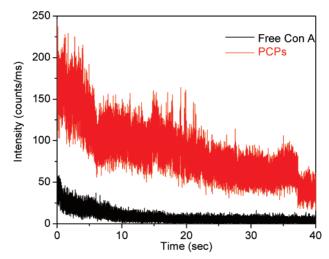
Figure 5. Respective time traces of unmodified con A and bound silver particles.

In order to understand the possible interactions between the metal particles and cells, we utilized the tiopronin-coated metal particles instead of PCPs in the incubation experiment. The metal particles were hardly observed near the cells after washing, implying that PCPs were conjugated on thee cultured cell basically through the interaction of bound con A instead of the silver particles. However, bulky PCPs may meet stronger steric hindrance when being proximate to and conjugating to the cells. The quantity of PCP on the cell surface must be less than that of unmodified con A. Because there is only one con A on each PCP, the quantity of fluorophore by PCP is proposed to be less than that by unmodified con A on the cell membrane. Therefore, the intensity enhancement of fluorescence on the cell images by PCPs is most probably attributed to the coupling effect among PCPs (*24*). In fact, when the metal particles are in close proximity to each other, the electric fields have been estimated to become more intensive due to overlapping from the individual fields (*50*), and the fluorophore localized in these overlapped fields is enhanced more efficiently (*43*). This result reveals that the signal intensity on the cell membrane can be enhanced not only as individually but more efficiently as coupled when PCPs are conjugated.

The coupling effect of PCPs also displays a better photostability on the cell membrane. Real-time intensity traces illustrate that almost half of the unmodified con A molecules on cells were bleached out in 5 s, while intensities of PCPs decay more gradually (Figure 7). If the fluorophores are supposed to be bleached proportionally with time as shown in the decay curves, we can propose that the photostability of PCPs on the cell membrane is at least 10 times longer than that of unmodified con A.

The coupling mechanism of fluorophore with metal particles can be discussed by lifetimes. It is known that the interaction between the fluorophore and metal particles can result in a dramatic change of radiating energy that is expressed as an apparent increase of intrinsic decay rate (*25*). Such an increase of intrinsic decay rate can be monitored by the lifetime of a fluorophore. In this study, the lifetime data were collected from the time traces using single molecule time-corrected single photon counting (TCSPC). The lifetime of unmodified con A was estimated to be 2.5 ns and furthermore shortened to be 1.2 ns when bound to the metal particles, affirming the existence of interaction between fluorophores and metal particles. When the fluorophore was associated on the cells as an unmodified state or PCP, the intensity was observed to decay differently in which the decay by PCP was more rapid than that by unmodified con A (Figure 8), and the lifetimes were estimated to be 1.1 ns (PCPs) and 2.4 ns (unmodified con A), respectively. It is uncertain why the lifetime did not further shorten when associating PCPs on the cells membrane. Many factors including the distance between the PCPs and environmental changes for the fluorophore, etc., may be partially responsible.

The tiopronin-coated metal particles with an average diameter of 20 nm were decorated quantitatively by Alexa Fluor 647-labeled con A in a molar ratio of 1:1 to generate metal plasmon-coupled probes (PCPs) as fluorescence imaging agents. HEK293 A cells were conjugated by PCPs and unmodified dye-labeled con A, respectively, and fluorescently imaged using scanning
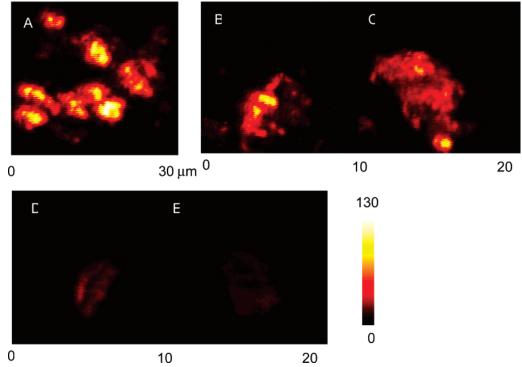

Figure 6. Representative fluorescent images of HEK 293 A cell lines (a−c) labeled by PCPs, and (d and e) labeled by unmodified con A.

Figure 7. Respective time traces from fluorescent images labeled by con A and PCPs on the cell membrane.
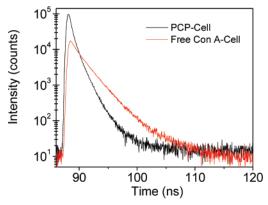

Figure 8. Respective TCSPC curves from fluorescent images labeled by unmodified con A and PCPs on the cell membrane.

confocal microscopy at the single cell level. The fluorescence images of cell lines by PCPs were 20 times brighter than those by unmodified con A, and the photostability was 10 times longer. These results reveal that the PCPs can work efficiently as brighter and more photostable imaging agents. In this case, the dye-labeled con A is only bound to the silver particles in a molar ratio of 1:1 for research convenience. Actually, with increasing the binding number of con A on each metal particle to an optimal value, PCP is supposed to be brighter up to hundreds of times than unmodified con A. The high number of con A on PCP can increase its capability to catch the target on the cell membrane. One metal particle can also be decorated readily by more than one kind of fluorophore, so multicolor PCP will be investigated in further work. In addition, PCP displays a longer photostability, so it can be utilized in long-range diagnosis and treatment of disease.

ACKNOWLEDGMENT

LITERATURE CITED

(1) Weissleder, R., Tung, C. H., Mahmood, U., and Bogdanov, A. (1999) In vivo imaging of tumors with protease-activated near-infrared fluorescent probes. *Nature Biotechnol. 17*, 375−378.

(2) Ntziachristos, V., and Chance, B. (2001) Probing physiology and molecular function using optical imaging: applications to breast cancer. *Breast Cancer Res. 3*, 41−46.

(3) Chen, I., and Ting, A. Y. (2005) Site-specific labeling of proteins with small molecules in live cells. *Curr. Opin. Biotechnol. 16*, 35−40.

(4) Howarth, M., Takao, K., Hayashi, Y., and Ting, A. Y. (2005) Targeting quantum dots to surface proteins in living cells with biotin ligase. *Proc. Nat. Acad. Sci. U.S.A. 102*, 7583−7588.

(5) Rosenthal, S. J., Tomlinson, I., Adkins, E. M., Schroeter, S., Adams, S., Swafford, L., McBride, J., Wang, Y., DeFelice, L. J., and Blakely, R. D. (2002) Targeting Cell Surface Receptors with Ligand-Conjugated Nanocrystals. *J. Am. Chem. Soc. 124*, 4586−4594.

(6) Vivero-Pol, L., George, N., Krumm, H., Johnsson, K., and Johnsson, N. (2005) Multicolor Imaging of Cell Surface Proteins. *J. Am. Chem. Soc. 127*, 12770−12271.

(7) Van Dijk, M. A., Lippitz, M., and Orrit, M. (2005) Far-Field Optical Microscopy of Single Metal Nanoparticles. *Acc. Chem. Res. 38*, 594−601.

(8) Shen, Y., Swiatkiewicz, J., Lin, T.-C., Markowicz, P., and Prasad, P. N. (2002) Near-Field Probing Surface Plasmon Enhancement Effect on Two-Photon Emission. *J. Phys. Chem. B 106*, 4040−4042.

(9) Yonzon, C. R., Jeoung, E., Zou, S., Schatz, G. C., Mrksich, M., and Van Duyne, R. P. (2004) A Comparative Analysis of Localized and Propagating Surface Plasmon Resonance Sensors: The Binding of Concanavalin A to a Monosaccharide Functionalized Self-Assembled Monolayer. *J. Am. Chem. Soc. 126*, 12669−12676.

(10) Yu, F., Persson, B., Lofas, S., and Knoll, W. (2004) Attomolar Sensitivity in Bioassays Based on Surface Plasmon Fluorescence Spectroscopy. *J. Am. Chem. Soc. 126*, 8902−8903.

(11) Lee, I.-Y. S., Suzuki, H., Ito, K., and Yasuda, Y. (2004) Surface-Enhanced Fluorescence and Reverse Saturable Absorption on Silver Nanoparticles. *J. Phys. Chem. B 108*, 19368−19372.

(12) Ekgasit, S., Thammacharoen, C., Yu, F., and Knoll, W. (2004) Evanescent Field in Surface Plasmon Resonance and Surface Plasmon Field-Enhanced Fluorescence Spectroscopies. *Anal. Chem. 76*, 2210−2219.

(13) Song, J.-H., Atay, T., Shi, S., Urabe, H., and Nurmikko, A. V. (2005) Large Enhancement of Fluorescence Efficiency from CdSe/ZnS Quantum Dots Induced by Resonant Coupling to Spatially Controlled Surface Plasmons. *Nano Lett. 5*, 1557−1561.

(14) Baluschev, S., Yu, F., Miteva, T., Ahl, S., Yasuda, A., Nelles, G., Knoll, W., and Wegner, G. (2005) Metal-Enhanced Up-Conversion Fluorescence: Effective Triplet-Triplet Annihilation near Silver Surface. *Nano Lett. 5*, 2482−2484.

(15) Kawasaki, M., and Mine, S. (2005) Enhanced Molecular Fluorescence near Thick Ag Island Film of Large Pseudotabular Nanoparticles. *J. Phys. Chem. B 109*, 17254−17261.

(16) Malicka, J., Gryczynski, I., Gryczynski, Z., and Lakowicz, J. R. (2003) Effects of Fluorophore-to-silver Distance on the Emission of Cyanine-dye-labeled Oligonucleotides. *Anal. Biochem. 315*, 57−66.

(17) Aslan, K., Huang, J., Wilson, G. M., and Geddes, C. D. (2006) Metal-Enhanced Fluorescence-Based RNA Sensing. *J. Am. Chem. Soc. 128*, 4206−4207.

(18) Antunes, P. A., Constantino, C. J. L., Aroca, R. F., and Duff, J. (2001) Langmuir and Langmuir-Blodgett Films of Perylene Tetracarboxylic Derivatives with Varying Alkyl Chain Length: Film Packing and Surface-Enhanced Fluorescence Studies. *Langmuir 17*, 2958−2964.

(19) Kumbhar, A. S., Kinnan, M. K., and Chumanov, G. (2005) Multipole Plasmon Resonances of Submicron Silver Particles. *J. Am. Chem. Soc. 127*, 12444−12445.

(20) Bruzzone, S., Malvaldi, M., Arrighini, G. P., and Guidotti, C. (2005) Theoretical Study of Electromagnetic Scattering by Metal Nanoparticles. *J. Phys. Chem. B 109*, 3807−3812.

(21) Hubert, C., Rumyantseva, A., Lerondel, G., Grand, J., Kostcheev, S., Billot, L., Vial, A., Bachelot, R., Royer, P., Chang, S.-h., Gray, S. K., Wiederrecht, G. P., and Schatz, G. C. (2005) Near-Field Photochemical Imaging of Noble Metal Nanostructures. *Nano Lett. 5*, 615−619.

(22) Kreibig, U., and Vollmer, M. (1995) *Optical Properties of Metal Clusters*, Springer Series in Materials Science, Vol. 25, Springer-Verlag, Berlin and Heidelberg, Germany.

(23) Lakowicz, J. R. (2006) *Principles of Fluorescence Spectroscopy*, 3rd ed., Kluwer Academic/Plenum Publishers, New York.

(24) Lakowicz, J. R. (2005) Radiative Decay Engineering 5: Metal-Enhanced Fluorescence and Plasmon Emission. *Anal. Biochem. 337*, 171−194.

(25) Lakowicz, J. R. (2001) Radiative Decay Engineering: Biophysical and Biomedical Applications. *Anal. Biochem. 298*, 1−24.

(26) Drexhage, K. H. (1974) *Progress in Optics XII* (Wolf, E., Eds.) North Holland: Amsterdam.

(27) Gryczynski, I., Malicka, J., Shen, Y., Gryczynski, Z., and Lakowicz, J. R. (2002) Multiphoton Excitation of Fluorescence near Metallic Particles: Enhanced and Localized Excitation. *J. Phys. Chem. B 106*, 2191−2195.

(28) Hayat, M. A. Ed. (1991) *Colloidal Gold: Principles, Methods, and Applications*; Academic Press, San Diego.

(29) Feldheim, D. L., and Foss, C. A. (2002) *Metal Nanoparticles. Synthesis, Characterization and Applications*, Marcel Dekker, Inc., New York.

(30) Templeton, A. C., Wuelfing, W. P., and Murray, R. W. (2000) Monolayer-Protected Cluster Molecules. *Acc. Chem. Res. 33*, 27−36.

(31) Kamat, P. V. (2002) Photophysical, Photochemical and Photocatalytic Aspects of Metal Nanoparticles. *J. Phys. Chem. B 106*, 7729−7744.

(32) Rosi, N. L., and Mirkin, C. A. (2005) Nanostructures in Biodiagnostics. *Chem. Rev. 105*, 1547−1562.

(33) Osella, D., Pollone, P., Ravera, M., Salmain, M., and Jaouen, G. (1999) Use of Heavy-Metal Clusters in the Design of N-Succinimidyl Ester Acylation Reagents for Side-Chain-Specific Labeling of Proteins. *Bioconjugate Chem. 10*, 607−612.

(34) Schuler, B., and Pannell, L. K. (2002) Specific Labeling of Polypeptides at Amino-Terminal Cysteine Residues Using Cy5-benzyl Thioester. *Bioconjugate Chem. 13*, 1039−1043.

(35) Barbarella, G., Zambianchi, M., Ventola, A., Fabiano, E., Della Sala, F., Gigli, G., Anni, M., Bolognesi, A., Polito, L., Naldi, M., and Capobianco, M. (2006) Bright Oligothiophene *N*-Succinimidyl Esters for Efficient Fluorescent Labeling of Proteins and Oligonucleotides. *Bioconjugate Chem. 17*, 58−67.

(36) Biran, I., and Walt, D. R. (2002) Optical Imaging Fiber-Based Single Live Cell Arrays: A High-Density Cell Assay Platform. *Anal. Chem. 74*, 3046−3054.

(37) Kelly, T. L., Lam, M. C. W., and Wolf, M. O. (2006) Carbohydrate-Labeled Fluorescent Microparticles and Their Binding to Lectins. *Bioconjugate Chem. 17*, 575−578.

(38) Ingram, R. S., Hostetler, M. J., and Murray, R. W. (1997) Poly-hetero-ω-functionalized Alkanethiolate-Stabilized Gold Cluster Compounds. *J. Am. Chem. Soc. 119*, 9175−9178.

(39) Zhang, J., Matveeva, E., Gryczynski, I., Leonenko, Z., and Lakowicz, J. R. (2005) Metal-Enhanced Fluoroimmunoassay on a Silver Film by Vapor Deposition. *J. Phys. Chem. B 109*, 7969−7975.

(40) Zhao, H.-F., Kiyota, T., Chowdhury, S., Purisima, E., Banville, D., Konishi, Y., and Shen, S.-H. (2004) A Mammalian Genetic System To Screen for Small Molecules Capable of Disrupting Protein-Protein Interactions. *Anal. Chem. 76*, 2922−2927.

(41) Mikolajczyk, J., Scott, F. L., Krajewski, S., Sutherlin, D. P., and Salvesen, G. S. (2004) Activation and Substrate Specificity of Caspase-14. *Biochemistry 43*, 10560−10569.

(42) Brust, M., Walker, M., Bethell, D., Schiffrin, D. J., Whyman, R. J. (1994) Synthesis of Thiol Derivatised Gold Nanoparticles in a Two-Phase Liquid/Liquid System. *J. Chem. Soc., Chem. Commun*. 801−802.

(43) Zhang, J., Malicka, J., Gryczynski, I., and Lakowicz, J. R. (2005) Surface-Enhanced Fluorescence of Fluorescein-Labeled Oligonucleotides Capped on Silver Nanoparticles. *J. Phys. Chem. B 109*, 7643−7648.

(44) Huang, T., and Murray, R. W. (2002) Quenching of [Ru(bpy)$_3$]$^{2+}$ Fluorescence by Binding to Au Nanoparticles. *Langmuir 18*, 7077−7081.

(45) Hicks, J. F., Miles, D. T., and Murray, R. W. (2002) Quantized Double-Layer Charging of Highly Monodisperse Metal Nanoparticles. *J. Am. Chem. Soc. 124*, 13322−13328.

(46) Schaaff, T. G., Shafigullin, M. N., Khoury, J. T., Vezmar, I., and Whetten, R. I. (2001) Properties of a Ubiquitous 29 kDa Au:SR Cluster Compound. *J. Phys. Chem. B 105*, 8785−8796.

(47) Zhang, J., Roll, D., Geddes, C. D., and Lakowicz, J. R. (2004) Aggregation of Silver Nanoparticle-Dextran Adducts with Concanavalin A and Competitive Complexation with Glucose. *J. Phys. Chem. B 108*, 12210−12214.

(48) Geddes, C. D., Parfenov, A., Gryczynski, I., and Lakowicz, J. R. (2003) Luminescent Blinking from Silver Nanostructures. *J. Phys. Chem. B 107*, 9989−9993.

(49) Zeng, L., Miller, E. W., Pralle, A., Isacoff, E. Y., and Chang, C. J. (2006) A Selective Turn-On Fluorescent Sensor for Imaging Copper in Living Cells. *J. Am. Chem. Soc. 128*, 10−11.

(50) Storhoff, J. J., Lazarides, A. A., Mirkin, C. A., Letsinger, R. L., Mucic, R. C., and Schatz, G. C. (2000) What Controls the Optical Properties of DNA-Linked Gold Nanoparticle Assemblies? *J. Am. Chem. Soc. 122*, 4640−4650.